Production Engineering (2025) 19:275–281
https://doi.org/10.1007/s11740-024-01309-8

ORIGINAL PAPER

Geometric physically-based simulation of microfinishing: tool design impact on workpiece shape

Tobias Siebrecht[1] · Jim A. Bergmann[1] · Ines Heining[1] · Meik Tilger[2] · Dirk Biermann[2] · Petra Wiederkehr[1,3]

Received: 17 January 2024 / Accepted: 4 September 2024 / Published online: 12 September 2024

Abstract
Due to complex interrelations between process configurations, tool characteristics and process results, the design of microfinishing operations is challenging. Microfinishing is often conducted to generate high surface qualities and shape accuracies of highly loaded components. For some applications, e.g. bearing seats, the contact surface is desired to provide a convex shape in order to optimise the contact condition of the bearing ring and the shaft shoulder. In this paper, new models for a geometric physically-based simulation system are presented and applied to predict workpiece topographies and shapes resulting from the use of different tool designs in microfinishing operations. These models include a process-specific force control based on modelling the engagement of single grains, the consideration of the initial tool condition as well as the modelling of wear-related breakouts of individual grains. The developed simulation system was validated by a comparison of the results to experimental investigations.

Keywords Modelling · Honing · Tool design · Geometric physically-based simulation

1 Introduction

Short stroke honing [1], also called superfinishing [2] or microfinishing, is often conducted to modify the workpiece surface concerning texturing and topography [2], generate surfaces without damages or heat-affected zones [2], adjust functional properties of highly loaded components, e.g., crankshaft bearings, eliminate shape deviations by improving the roundness [3] and enhancing the noise emission of components like bearings or gearboxes by reducing vibrations [4]. Depending on the workpiece geometry, material, initial roughness as well as target topography, different tool types can be used [2]. Such tools can be characterized by, e.g., cutting material, grain size and bond material. In order to achieve a desired functional behaviour of the workpiece, a suitable tool type and appropriate process parameter values need to be identified [5]. Due to complex interrelations between tool specifications, process parameter values and process results, which are also influenced by the run-in behaviour of the tool, grain wear and bond contact, a deep process knowledge and a large number of experiments are often required [6].

In order to design economically feasible processes by reducing the number of experiments, shortening the run-in phase by adapted process strategies [7] and gaining further understanding of the process [8], the use of simulation systems can be beneficial. Simulations of honing operations known in literature include different models for the representation of specific aspects of the honing process [2]. These aspects, such as process forces [6], material removal rate [9] or surface topography [10], can be modelled using, e.g., geometric-kinematic [11], geometric physically-based [8], numerical [12], empirical-analytical [13] or statistical models [9]. Furthermore, such aspects can be considered in macroscopic [14], mesoscopic [5] or microscopic scale [12]. Goeldel et al. [14] presented a macroscopic approach for the simulation of an overall long-stroke finishing process of cylinder liners. In the simulation, process parameters like the number of strokes or cycle time could be adjusted in

✉ Jim A. Bergmann
jim.bergmann@tu-dortmund.de

1 Virtual Machining, TU Dortmund University, Otto-Hahn-Straße 12, Dortmund 44227, Germany

2 Institute of Machining Technologie, TU Dortmund University, Baroper Straße 303, Dortmund 44227, Germany

3 Lamarr Institute for Machine Learning and Artificial Intelligence, TU Dortmund University, Joseph-von-Fraunhofer-Straße 25, Dortmund 44227, Germany

Production Engineering (2025) 19:275–281

order to achieve a requested form quality and roughness of the bore surface [14]. In addition, stock removal and a map of remaining stock could be determined in order to identify an optimised tool geometry and honing kinematics [14]. A statistical model for the determination of surface roughness values and the material removal rate in rough honing was presented by Buj-Corral et al. [9]. A multi-objective optimisation was used in the model in order to select suitable honing conditions. Thus, process parameter values could be adjusted resulting in high material removal rates combined with a low surface roughness. Karpuschewski et al. [12] developed a numerical modelling approach to optimise the finishing process of cylinder running surfaces. In the simulation, microscopic and macroscopic effects on the process were considered seperately. The occurring process forces were identified as significant influence on the characteristics of the inner and outer boundary layer of the cylinder running surface in combustion engines. Bergs et al. [13] calculated the cutting force occurring from gear honing processes by using an empirical-analytical model. In gear honing processes the tool is dressed during tool life resulting in constantly varying dressing conditions of the tool. For this reason local cutting forces were determined by conducting analogy processes using analogy tools that were conditioned with three different cross axis angles. The cutting force was calculated with a modified grinding force model developed by [15]. In previous investigations [8], a mesoscopic geometric physically-based honing simulation was developed for modelling a force-controlled microfinishing process using a finishing belt. In order to predict and analyse the resultig surface topography, tool and workpiece were modelled as heightfields. In order to provide a time efficient calculation of the simulation results, only a small part of the tool topography was modelled explicitly. To achieve more realistic results concerning the surface topograhy of the workpiece, burr formation was modelled, as well, by using second order approximation functions for the calculation of the plastic deformation of the material on a microscopic scale during single grain cutting [16]. Burr formation was identified by using Coupled Eulerian-Lagrangian method in a single grain FE-model. In this model, also the grain geometry, the depth of cut and the undeformed chip thickness were taken into account and the approximation functions describing the burr formed from the cut were determined. Subsequently, material was added to the surface next to the cutting area using a bounding box around the engagement area of the grain and the workpiece in the geometric physically-based simulation. As a result, burr formation could be represented in the process simualtion, as well [16]. The aim of the presented investigations is the development of a process simulation for the evaluation of the influence of different tool designs on the resulting workpiece surface. For this purpose, novel simulation models are required that allow for a high-resolution prediction of the workpiece shape and topography resulting from the microfinishing process depending on the design of the abrasive stones. These models have to adequately represent

- a process-specific force control based on individual grains,
- the initial condition of the tool and
- tool wear

with appropriate efficiency regarding run-times.

2 Modelling the microfinishing process

In the following, such a simulation system for the analysis of microfinishing processes is presented. For this purpose, a novel tool model based on the geometric description of individual grains of the metal-bonded diamond tools was developed. Since the resulting workpiece shape is influenced by tool wear, the wear behaviour of the tools was analysed and modelled. The self-sharpening effect of the microfinishing tools was taken into account by modelling wear-related breakouts of the abrasive grains. As an exemplary application, this simulation system was used to investigate the influence of the shape of conventional abrasive stones (Fig. 1a, T1) and a specifically modified tool design (T2) on the resulting workpiece shape.

2.1 Experimental Setup

In order to develop the required models, appropriate experiments had to be conducted. As an application case, the microfinishing of shaft shoulders with a diameter of $d_w = 54.2$ mm and a width of $w_w = 13$ mm was investigated (cf. Fig. 1b). The workpiece material was 16MnCr5, case hardened to approximately 58 HRC. In order to obtain a homogeneous workpiece surface, the shaft shoulders were preliminary ground ($Rz = 3.1$ µm). Subsequently, the microfinishing experiments were conducted on a cylindrical grinding machine (RS 600 C CL, Geibel & Hotz). The

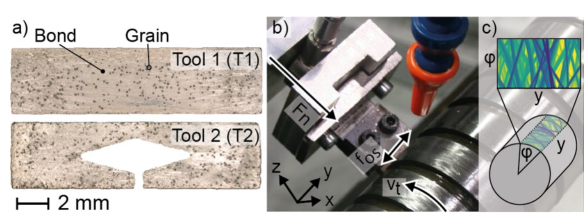

Fig. 1 Experimental setup showing **a** the tool designs (T1 and T2), **b** the process kinematic (oscillation frequency f_{os}; workpiece velocity v_t; pneumatically realised normal force F_n) and **c** the model of the workpiece using cylindrical projection

workpiece rotation was superimposed with an oscillation of the tool in y-direction (cf. Fig. 1b), resulting in the effective cutting velocity v_c. A stone microfinishing device (SG 50, NAGEL) was utilised to generate a constant normal force F_n by pneumatically controlling the tool in z-direction normal to the workpiece. The superimposed oscillation of the tool along the shaft shoulder (y-direction) was established by pneumatic pressure (cf. Fig. 1b) and the generated oscillation amplitude was verified for each experiment using a laser displacement measurement system (LK-G32, Keyence). The specific process parameter values for the initialisation and validation experiments are described in Sects. 3 and 4, respectively. To record the occurring process forces, a 3-component force measuring element (9017C, Kistler) was integrated in the tool holder. For lubrication, a honing oil (Honilo 981, Castrol) was applied to the engagement area. Microfinishing stones with metallically bonded D126 diamond grains were used in the experiments. In order to analyse the influence the shape of the shaft shoulders, two different tool designs were applied (cf. Fig. 1a)—a conventional microfinishing stone (T1) and a stone with a diamond-shaped cavity (T2, prototype, ELGAN) to achieve a convexity on the shaft shoulders after the process. In order to consider the distribution of the grains within the volume and the wear progression of the tools in the process, the development of a novel tool model was necessary, which is presented in Sect. 2.2.

A further challenge was the accurate modelling of the process forces and the simulation of a constant pressure, requiring a control loop for varying the effective depth of cut to maintain constant process forces as described in Sect. 2.3.

2.2 Wear-dependent tool model for arbitrary microfinishing stones

Based on the idea of an explicit geometric description of individual grains for the simulation of grinding processes [17], a stochastic tool model was developed for the representation of the grain distributions within the bond of the microfinishing stones. This has enabled the possibility of modeling the modification of the tool through the removal of grains in order to take into account the wear-related change in tool shape during machining. This modeling approach is essential in order to describe the mechanisms underlying the process for producing workpiece topographies. For the parameterization of this model, several investigations were conducted. In order to consider tool wear in the model, several shaft shoulders were finished with the tool designs T1 and T2 with a nominal pressure of $P = 3$ bar. For the generation of a database of representative grain shapes, the microfinishing stones were digitised before and after the experiments using a 3D measuring system (Infinite Focus G5, Alicona). The tool topographies after the

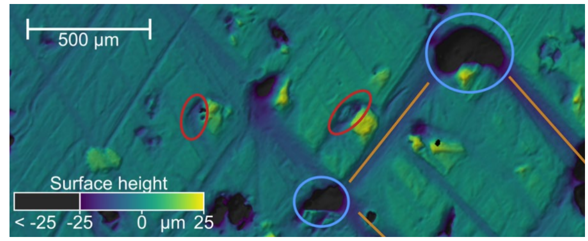

Fig. 2 Wear state of an exemplary microfinishing stone with grain breakouts (blue), grooves (orange) and crater wear (red) after the run-in phase

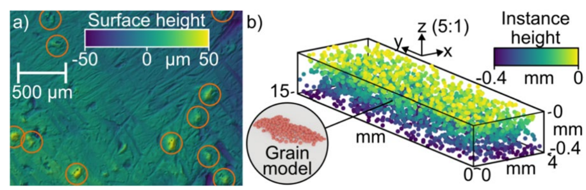

Fig. 3 **a** Measurement of a microfinishing stone with exposed grains (orange). **b** Generated grain instances in the considered section of the tool volume, each represented by point clouds

processes—an example is presented in Fig. 2—show cavities of grain breakouts (blue) with partly appearing grooves within the bond along the breakout path (orange). In addition, crater wear occured at several grains in the effective cutting direction (red), which presumably was eroded around the grain during chip removal. For the simulation of the process, these effects had to be taken into account in the tool model. Due to the breakout of grains and wear of the bond, new and sharp grains were exposed. In order to model individual grains explicitly, a grain database of grain models with representative grain shapes was developed on the basis of the digitized tool topographies. Thus, individual grains were segmented from the measurements prior to the finishing process (Fig. 3a) and stored using unstructured point clouds (Fig. 3b) [17]. Subsequently, these grain models were homogenously placed in the volume of the bond in defined areas of the tool by using a function of statistical distribution. The described database approach provided the flexibility to use the individual grain models for arbitrary tool sizes and shapes. Although it is possible to generate the grain distribution in the full volume of the tool, only the region up to 0.4 mm below the surface was modelled for the considered process to increase the simulation efficiency. As shown in the example in Fig. 3b), 2395 grain instances were generated for this section of the microfinishing stone with a width of 15 mm and a height of 4 mm. Since the macroscopic shape of the tools can deviate from an ideal tool shape, e.g., due to convexity, and this strongly influences the finishing result, the consideration of the initial tool condition in the simulation model was essential. For this purpose, the individual tool topographies were measured and analysed prior to the processes and the grain instances in the model were offset accordingly. For considering the observed wear effects in the new tool model, grains had to be removed according to their load occurring during the process. A tool wear coefficient v_{lim} was defined, which corresponded to the maximum volume of material that each grain could remove before it is torn out. Thus, tool wear was considered by removing grains from the tool model when v_{lim} was exceeded. The contact between bond and workpiece was not explicitly taken into account for this purpose.

Additionally, an immediate breakout was simulated when an undeformed chip thickness above 10 µm was detected, which led to breakouts in the preliminary experiments. The coefficients of the wear model were determined heuristically for the presented investigations (cf. Sect. 3).

2.3 Modelling of process forces and force control

In order to utilise the described tool model, the workpiece was modelled using heightfields, which have already been used successfully for the simulation of NC grinding processes [8, 17]. To apply this approach to the modelling of rotating cylindrical workpiece surfaces, cylindrical coordinates were used in the simulation system (Fig. 1c). In this coordinate system, the heightfield of the workpiece surface resembled a regular grid of height values, simplifying the required calculations and the implementation of the kinematics of the process. For this purpose, a rotary movement of the shaft and an oscillation of the tool lateral to the direction of rotation were carried out. These superimposed motions were represented planarly by a linear lateral forward motion coupled with a sinusoidal upward and downward motion corresponding to the amplitude and frequency of the stroke. The infeed movement was applied using a vertical displacement of the tool model. In order to simulate the change in the workpiece topography, the workpiece was modelled as a height field and was intersected with the individual grain models in each simulated time step. The undeformed chip thickness for the individual grains was determined for each time step, in order to calculate the process forces. Since the positions of the grain were also discretized by the time step, the cut volume between the individual grain positions during the cutting process were calculated with a sweep volume, which was projected onto the heightfield of the workpiece. These differences result in a course of maximum chip thicknesses for each grain within a time step, which can then be used for the process force calculation. The application of these sweep volumes changes the surface topography using erosion and dilatation filters to ensure the simulation of a continuous engagement of the grains, as described in [17]. However, it was necessary to develop a feedback control system that reproduced the load occurring in the process. In order to determine the process forces, the undeformed chip shape of each individual grain engagement was analysed with respect to the undeformed chip area A_{cu} [17]. By using a linear empirical force model [17] with the process force coefficients k_c and k_n in cutting and normal direction, the process forces were determined as $F_n = k_n \cdot A_{cu}$ and $F_c = k_c \cdot A_{cu}$ in the respective directions. A summation of these individual grain forces resulted in an estimate of the overall forces. In order to parameterise the empirical linear force model used, single-grain scratch tests were carried out in advance for diamond grains (D126) on specimens consisting of 16MnCr5. For three different isolated grains, experiments including repeated tests with infeeds between $a_e = 1$ µm and 5 µm were conducted respectively. Different engagement depths were then extracted from the measurements, which were used to regressively determine the coefficients of the model (Fig. 4). According to these results, the process force coefficients for the individual grain engagements were determined as $k_c = 50370\,\mathrm{Nmm}^{-2}$ and $k_n = 122584\,\mathrm{Nmm}^{-2}$. Due to the fact that the shaft was machined evenly over the entire revolution, it was sufficient to consider only a small section of the shaft circumference during the process simulation without neglecting necessary information. However, the section should be large enough to cover a full tool overlap. This is essential to allow a sufficient contact of the engaged grains for the determination of the process forces required for force control. Therefore, the forces were calculated at a complete overlap of the workpiece-tool interaction. To achieve an engagement depth corresponding to the target pressure in the simulation, the infeed was iteratively adapted until the target force was reached for each workpiece rotation. For the determination of grain breakouts, the material removed was stored for each grain during the engagements.

3 Simulation of different tool designs

In order to analyse the potential of the developed simulation system for predicting the resulting workpiece shapes and surface topographies, investigations were carried out on different tool designs, which are discussed in the following using the examples T1 and T2 (cf. Fig. 1a). The conventional tool design T1 is characterised by a uniform grain

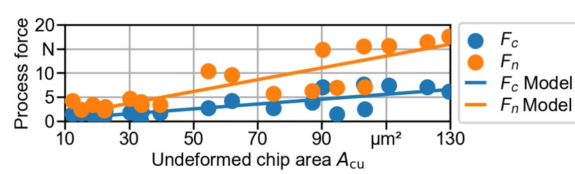

Fig. 4 Process forces determined in single-grain scratch tests with different undeformed chip areas in comparison to the simulated forces

distribution to achieve a homogeneous surface finish. Tool design T2 was used to achieve a convex shape of the shaft shoulder. The developed simulation system was applied for both tool designs. According to typical industrial applications, a reference force of $F_n = 300\,\mathrm{N}$, an oscillation amplitude of $A_{os} = 3\,\mathrm{mm}$ with a frequency of $f_{os} = 35\,\mathrm{Hz}$ and a tangential velocity of $v_c = 51\,\mathrm{m\,min}^{-1}$ were considered. A process duration of $t = 10\,\mathrm{s}$ was analysed, which is common for these processes [18]. The analysed process configurations were simulated using the novel approach with run times below one minute on a mobile workstation. In order to consider the forces resulting from the bond contact, which was not modelled explicitly, it was assumed that 60 % of the measured total forces resulted from grain engagements and 40 % from bond contact, estimated based on the grain distribution. Regarding the modelled force control, this simplification led to a target peak force of $F_n = 180\,\mathrm{N}$ (i.e. 60 % of 300 N). In circumferential direction, 4 mm of the workpiece surface were modelled, corresponding to 2.35 % of the real surface area, using a heightfield resolution of 0.01 mm. A tool wear coefficient of $v_{\lim} = 0.03\,\mathrm{mm}^3$ was found to be adequate in the course of the investigations. With respect to the modelled section of the workpiece surface, this corresponded to a removed material volume of approximately $V_w = 1.278\,\mathrm{mm}^3$ in the real process. The simulated surface topographies (Fig. 5) show a formation of cross grooves, which is characteristic for microfinishing processes. Furthermore, a significant influence of the tool design on the shape of the resulting surface was observed. Using tool type T2, a surface with a convex shape was achieved, which was validated as described in Sect. 4.

4 Experimental validation

For the validation of the presented simulation model, microfinishing experiments were conducted (cf. Fig. 1) with varying process times t of 10 s, 15 s and 20 s for T1 and T2, respectively. Analogous to the initialisation experiments (cf. Sect. 2.2), the pressure was also set to $P = 3$ bar. The oscillation unit of the tool was adjusted to achieve an oscillation amplitude of $A_{os} = 3\,\mathrm{mm}$ with a frequency of $f_{os} = 35\,\mathrm{Hz}$. Since the oscillation amplitude was reduced by up to 27 % during tool engagement, the effective amplitudes were determined based on process measurements and used in the simulations. An exemplary measurement of process forces is depicted in Fig. 6, showing a force of approximately $F_t = 300\,N$ acting on the tool in z-direction and the force peaks resulting from the force control in the simulation. According to the measured initial macroscopic shape of the tool T1, a convexity of approximately 10 μm was applied to the corresponding tool model by offsetting the grains as described in Sect. 2.2. Furthermore, each of the processes was simulated with ten different randomised grain distributions to adequately represent the stochastic character of the process. Exemplary resulting surface topographies, digitised using the 3D measuring system, are shown in Figs. 7a and 8a as well as the averaged surface profiles in Figs. 7b and 8b. While all simulated surface profiles for each of the ten stochastically generated grain distributions are shown in grey,

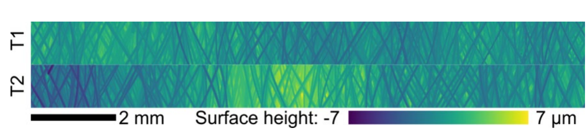

Fig. 5 Surface topographies simulated using a conventional tool design (T1) and a tool with a diamond-shaped cavity (T2). The formation of a convexity can be observed when using T2

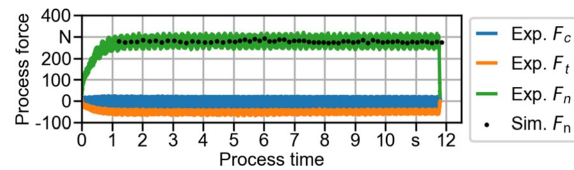

Fig. 6 Simulated force peaks of the force control in comparison to the measured forces

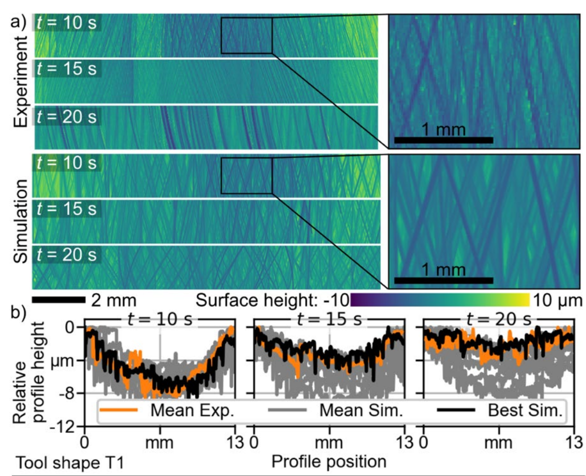

Spindle speed	n = 15915 min^{-1}	Workpiece diameter	d_w = 54.2 mm
Normal force	F_n = 300 N	Oscillation amplitude	A_{os} = ±1.5 mm
Oscillation frequency	f_{os} = 35 Hz	Cutting Speed	v_c = 0.85 ms^{-1}

	Experiment		Simulation	
For t = 10 s :	Rz = 6.66 μm	Ra = 1.12 μm	Rz = 6.19 μm	Ra = 1.15 μm
For t = 15 s :	Rz = 4.02 μm	Ra = 0.73 μm	Rz = 5.69 μm	Ra = 0.98 μm
For t = 20 s :	Rz = 6.29 μm	Ra = 1.18 μm	Rz = 5.49 μm	Ra = 0.95 μm

Fig. 7 **a** Measured and simulated surface topographies for considered process durations using tool design T1 with **b** corresponding average surface profiles

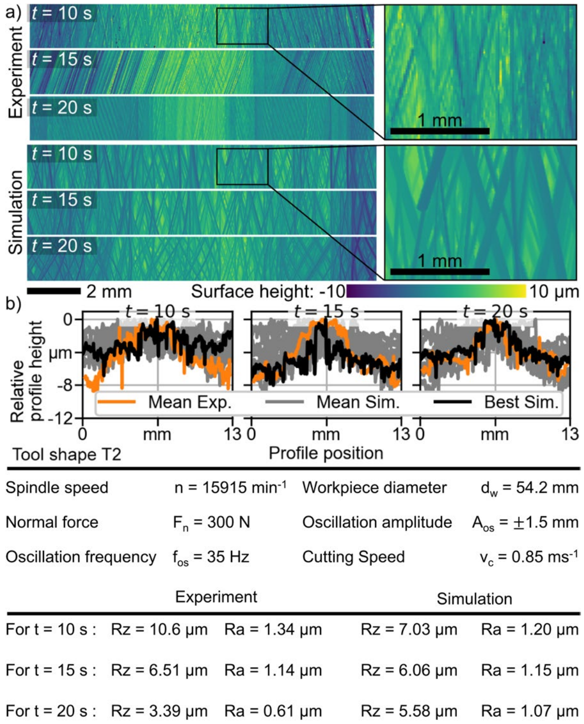

Fig. 8 **a** Measured and simulated surface topographies and **b** corresponding average surface profiles using tool design T2

the one with the best agreement with the experiments was highlighted for each case (black).

The simulation results show the same correspondence between the tool design, process duration and shape of the resulting workpiece surface as the experiments. The uniform grain distribution of the conventional tool design T1 should result in a homogeneous workpiece surface, while T2 was designed to ensure a convex surface shape. The topographies shown in Fig. 7a correspond to the highlighted profiles in Fig. 7b (black). The effects observed in the experiments were predicted by the simulation, although the exact surface topography contained deviations due to the simulated grain distribution and assumptions made. In some cases (e.g. $t = 15$ s), the simulated roughness was higher, which can be explained by the neglect of effects like elastoplastic material deformation and the assumptions made regarding the contact between the bond and the workpiece surface in the simulation system. As can be seen in Fig. 7b, the experiments (orange) using T1 resulted in a concave surface shape due to the initial condition of the tool. By considering this tool condition also in the simulation model (c.f. Sect. 2.2), this effect could be predicted (Fig. 7b). With increasing process duration t, this concavity was reduced. However, a convex surface was not achieved even after 20 s.

As expected from the initial simulation results (Fig. 5), a distinct convex shape was obtained using tool design T2 with the diamond-shaped cavity (Fig. 8). The occurrence of concavities was prevented by all ten selected grain distributions, although the degree of pronounced convexity varied (Fig. 8b, grey). The effect of grain breakouts is more dominant for T2 compared to T1, since the shape of T1 is a full rectangle and not modified by cutouts. Thus, T1 has a higher degree of overlap of the tool surface during the process compared to T2 and a higher material removal rate. For this reason, the stochastic character of the grain distribution and the occuring tool wear can be more significant for short process times than for longer process times. This explains the initial deviation of the results for the process time of $t = 10$ s shown in Fig. 8. Furthermore, grain breakouts were considered as the only wear mechanism of the tool, since the bond was not explicitly modeled. However, other wear mechanisms that can be assigned to the bond could also have an effect in the process and might lead to deviations in the simulation results. Evaluating the symmetry of the convexity, it can be seen that at $t = 10$ s profile deviations of 2.5 µm and 1 µm still occur at the edges, whereas at $t = 15$ s and $t = 20$ s only deviations of under 1 µm on each side occured and had a sufficiently comparable width. Overall, a minor deviation was achieved for higher process durations, with slight convexity deviations for $t = 10$ s.

5 Conclusion and outlook

In this paper, a geometric physically-based simulation system for the analysis of microfinishing processes with metal-bonded microfinishing stones was presented. By modelling the 3-dimensional distribution of individual grains and tool wear effects (breakouts), surface topographies and workpiece shape were predicted. The simulation system was exemplarily applied to analyse the influence of two different tool designs on the resulting shape of shaft shoulders for bearing seats. In order to achive a beneficial contact area between a bearing ring and the shaft shoulder, different tool designes (T1 and T2) were investigated with regard to the resulting shape of the shaft shoulder. It could be shown that a diamond-shaped cavity led to the desired convex shape of the surface profiles and an experimental validation showed a good correspondence between simulation results and measured surface topographies for higher process times. Future work will especially be focussed on the conduction of further experiments for different tool designs and grain sizes in order to achieve an efficient parametrisation of the simulation models and the development of a more detailed model of the tool including the explicit representation of the bond. Additionally, wear mechanisms of the microfinishing tool including bond wear and grain wear will be further investigated in order to achieve a better understanding of the tool wear progress and occurring types of wear, e. g. grain splintering or crater wear of the bond. The simulation system can then be used to analyse the influence of different grain sizes, topographies and shapes of the tool on the resulting surface roughness and shape.

Acknowledgements We would like to thank Bruker Alicona, ELGAN Diamantwerkzeuge GmbH & Co. KG and NAGEL Maschinen- u. Werkzeugfabrik GmbH for their support.

Funding Open Access funding enabled and organized by Projekt DEAL. Gefördert durch die Deutsche Forschungsgemeinschaft (DFG) - 450792335. Funded by Deutsche Forschungsgemeinschaft (DFG, German Research Foundation) - 450792335. Additionally, the investigations are based on the research project "Virtual Machining" (PE-216-0024), which is kindly funded by the Stiftung Mercator and the Mercator Research Center Ruhr. The authors declare that no further funding was received during the preparation of the manuscript.

Data availability The data on which the results in this article are based cannot be made accessible for reasons of confidentiality.

Declarations

Conflict of interest The authors have no relevant financial or non-financial interests to disclose.

References

1. Uhlmann E, Spur G, Kleinschnitker M (2015) Honing and superfinishing, 1
2. Hashimoto F, Yamaguchi H, Krajnik P, Wegener K, Chaudhari R, Hoffmeister H-W, Kuster F (2016) Abrasive fine-finishing technology. CIRP Ann 65(2):597–620
3. Marinescu I, Dontu G, Bordeianu E (1998) High efficiency superfinishing of bearing rings with CBN. Technical papers of NAMRI/SME, pp 27–32
4. Beran J, Bílek M, Žabka P(2017) Advances in mechanism design II: proceedings of the XII international conference on the theory of machines and mechanisms, vol 44. Springer International Publishing, Cham
5. Joliet R, Kansteiner M, Kersting P (2015) A process model for force-controlled honing simulations. Procedia CIRP 28:46–51
6. Karpuschewski B, Goldau H, Stolze R (2014) Process force and technology model for designing and controlling finishing operations with rotating grinding tools. CIRP Ann 63(1):337–340
7. Goeke S, Biermann D, Stickel D, Stemmer P, Fischer A, Geenen K, Huth S, Theisen W (2014) Enhancing the surface integrity of tribologically stressed contacting surfaces by an adjusted surface topography. Procedia CIRP 13(Supplement C):214–218
8. Kersting P, Joliet R, Kansteiner M (2015) Modeling and simulative analysis of the micro-finishing process. CIRP Ann 64(1):321–324
9. Buj-Corral I, Vivancos-Calvet J, Coba-Salcedo M (2014) Modelling of surface finish and material removal rate in rough honing. Precis Eng 38(1):100–108
10. Görög A (2021) Simulation of superfinished surface formation. Adv Sci Technol Res J 15(2):219–227
11. Vargas GE, Wegener K, Kuster F, Schroeter RB (2014) Simulation of the hone broaching process with diamond tools. J Braz Soc Mech Sci Eng 36(2):325–333
12. Karpuschewski B, Welzel F, Risse K, Schorgel M, Kreter S (2016) Potentials for improving efficiency of combustion engines due to cylinder liner surface engineering. Procedia CIRP 46:258–265
13. Bergs T (2018) Cutting force model for gear honing. CIRP Ann 67(1):53–56
14. Goeldel B, El Mansori M, Dumur D (2012) Macroscopic simulation of the liner honing process. CIRP Ann 61(1):319–322
15. Bock R(1987) Schleifkraft modell für das außen- und innenrundschleifen. In: Saljé E (ed) Tagungsband zum 5. Internationalen Braunschweiger Feinbearbeitungskolloquium. Braunschweig
16. Wiederkehr P, Grimmert A, Heining I, Siebrecht T, Wöste F (2023) Potentials of grinding process simulations for the analysis of individual grain engagement and complete grinding processes. Front Manuf Technol 2:1102140
17. Wiederkehr P, Siebrecht T, Potthoff N (2018) Stochastic modeling of grain wear in geometric physically-based grinding simulations. CIRP Ann 67(1):325–328
18. Puthanangady TK (1995) Experimental investigation of the superfinishing process. Wear 185(1–2):173–182